

Two-Proton Correlations from 14.6A GeV/c Si+Pb and 11.5A GeV/c Au+Au Central Collisions

J. Barrette⁴, R. Bellwied⁸, S. Bennett⁸, R. Bersch⁶, P. Braun-Munzinger², W. C. Chang⁶, W. E. Cleland⁵, M. Clemen⁵, J. Cole³, T. M. Cormier⁸, Y. Dai⁴, G. David¹, J. Dee⁶, O. Dietzsch⁷, M. Drigert³, K. Filimonov⁴, S. C. Johnson⁶, S. Gilbert⁴, J. R. Hall⁸, T. K. Hemmick⁶, N. Herrmann², B. Hong², C. L. Jiang⁶, Y. Kwon⁶, R. Lacasse⁴, Q. Li⁸, T. W. Ludlam¹, S. K. Mark⁴, R. Matheus⁸, S. McCorkle¹, J.T. Murgatroyd⁸, D. Miśkowiec², E. O'Brien¹, S. Y. Panitkin⁶, V. S. Pantuev⁶, P. Paul⁶, T. Piazza⁶, M. Pollack⁶, C. Pruneau⁸, M. N. Rao⁶, E. Reber³, M. Rosati⁴, J. Sheen⁸, N. C. daSilva⁷, S. Sedykh⁶, U. Sonnadara⁵, J. Stachel⁹, H. Takai¹, E. M. Takagui⁷, S. Voloshin^{5,9}, T. Vongpaseuth⁶, G. Wang⁴, J. P. Wessels⁹, C. L. Woody¹, N. Xu⁶, Y. Zhang⁶, Z. Zhang⁵, C. Zou⁶ (E814/E877 Collaboration)

¹ Brookhaven National Laboratory, Upton, NY 11973

² Gesellschaft für Schwerionenforschung, Darmstadt, Germany

³ Idaho National Engineering Laboratory, Idaho Falls, ID 83402

⁴ McGill University, Montreal, Canada

⁵ University of Pittsburgh, Pittsburgh, PA 15260

⁶ SUNY, Stony Brook, NY 11794

⁷ University of São Paulo, Brazil

⁸ Wayne State University, Detroit, MI 48202

⁹ Physikalisches Institut der Universität Heidelberg, Heidelberg, Germany

(August 18, 2018)

Two-proton correlation functions have been measured in Si+Pb collisions at 14.6 AGeV/c and Au+Au collisions at 11.5 AGeV/c by the E814/E877 collaboration. Data are compared with predictions of the transport model RQMD and the source size is inferred from this comparison. Our analysis shows that, for both reactions, the characteristic size of the system at freeze-out exceeds the size of the projectile, suggesting that the fireball created in the collision has expanded. For Au+Au reactions, the observed centrality dependence of the two-proton correlation function implies that more central collisions lead to a larger source sizes.

PACS numbers: 25.75.-q, 25.75.Gz

I. INTRODUCTION

Measurements of two-particle relative momentum correlations [1,2] are widely used in relativistic heavy-ion physics as a tool for extracting information about the spatial and temporal extent of the system at freeze-out. The complexity of heavy-ion reactions demands the utilization of different particles as probes of the reaction zone in order to obtain a reliable picture of the collision. Most of the published experimental data are measurements of two-meson (π or K) [3–7] correlation functions while the information concerning baryon freeze-out configurations is far more sparse. Several methods have been suggested to address this problem: two-proton interferometry [8,9], analysis of the deuteron to proton yield ratios [10] and deuteron-proton interferometry [11,12]. In this paper we present measurements made by the E814/E877 collaboration at the BNL AGS of two-proton correlation functions in Si+Pb collisions at 14.6 AGeV/c and Au+Au collisions at 11.5 AGeV/c bombarding energy. The results of the two-pion correlation analysis for these systems were published in [5,13]. There, it was shown that pions at freeze-out, i.e. when the system is dilute enough so that no further strong interactions take place, originate from a source which significantly exceeds in size the projectile. Although the pion source is, through the strong pion-nucleon interaction, closely coupled to the baryon dynamics, a direct measurement of the source size of baryons at freeze-out via two-proton correlations is clearly important.

Two-proton correlations are due to the attractive strong and repulsive Coulomb final state interactions and are also influenced by the effects of quantum statistics which requires an antisymmetrization of the two-proton wave function. Coulomb repulsion, together with antisymmetrization, decreases the probability of detection of pairs with relative momentum close to zero, while the strong interaction increases this probability. The interplay of these effects leads to a characteristic “dip+bump” shape of the correlation function. The height of the peak of the correlation function can be related to the space-time parameters of the emitting source [8]. Thus an interpretation of the proton correlation data necessarily involves calculations of the final state interactions and assumptions about the properties of the emitting system. It has been shown [8,9] that, for simple static sources, the height, by which the peak deviates from unity, scales approximately inversely proportional to the source volume. However, in heavy-ion collisions, a direct determination of the source parameters from the proton correlation function is far from being straightforward. The

existence of collective effects [5,14,15], which leads to dynamical correlations between the momentum and position of the emitted hadrons, may create a situation in which the correlation function does not reflect the actual size of the source [5,16]. Under these conditions, utilization of a static source model [17] to generate the correlation and extract source parameters can be misleading. It seems necessary to utilize models, hydro-dynamical or transport, which attempt to describe collective effects to interpret the proton correlation functions. In order to deduce source parameters from the measured proton correlation functions, a transport model was used in the present analysis.

II. EXPERIMENTAL SETUPS

A. E814 Experimental Setup

Data used in the Si+Pb analysis were obtained with the E814 apparatus during the 1991 run. Detailed description of the experimental set up can be found in Ref. [5]. The apparatus consisted of several detector groups. A set of two high granularity calorimeters, Target Calorimeter (TCAL) and Participant Calorimeter (PCAL), positioned around the target area provided event by event measurements of transverse energy (E_T) production in the interval of pseudo rapidity $-2.0 < \eta < 4.7$. This measurement was supplemented by the data from a uranium calorimeter, located downstream of the forward spectrometer, which covered angles close to zero degrees, thus providing the experiment with the capability of almost 4π measurement of E_T . Global event characterization was also performed by a set of silicon multiplicity detectors each segmented into 512 pads and covering the pseudo rapidity range $0.8 < \eta < 3.9$. These detectors provided input for the trigger system. Note that the trigger was based on global event characteristics such as transverse energy production and charged particle multiplicity in a wide interval of pseudo rapidity. A high-resolution forward magnetic spectrometer was used for registration and identification of charged particles. The spectrometer had a rectangular aperture, with the beam passing through it, covering angles $-115 < \theta_x < 14$ mr in the magnetic bend (horizontal) plane, and $-21 < \theta_y < 21$ mr in the perpendicular plane [18,19]. The corresponding coverage in proton transverse momentum (p_t) and rapidity (y) is shown in Fig. 1. The 1991 configuration of the spectrometer consisted of a dipole magnet, two drift chambers and two time of flight (TOF) hodoscopes. The drift chambers were located at 7 (DC2) and 11.5 (DC3) meters downstream of the target. The position resolution of the drift chambers in the x direction was approximately $250 \mu\text{m}$ and $300 \mu\text{m}$, respectively. The hodoscopes were located at 12 and 31 meters downstream from the target with a time of flight resolution of 200 and 350 ps respectively. A group of detectors, located upstream of the target, consisting of a set of plastic scintillators and silicon detectors, provided information about beam particles and generated a start signal for the TOF system. Singly charged particles were selected by cuts on the amplitude of the signal in the TOF hodoscopes. Simultaneous measurements of the particle rigidity and time of flight in the spectrometer provided proton identification up to the momentum of the beam. In order to decrease multiple scattering and improve momentum resolution most of the space between the detectors in the forward spectrometer was filled with helium gas. The momentum resolution, found from the Monte Carlo studies, was better than 4.1% and is limited by multiple scattering. The invariant relative momentum (q_{inv} defined below) resolution was estimated to be on the order of 11 MeV/c for $q_{inv} \leq 40$ MeV/c (the most important region for the correlation measurement).

B. E877 Experimental Setup

The E877 apparatus was an upgrade of the E814 setup, designed to study central Au+Au collisions at about 11 AGeV/c. For a more detailed description see Ref. [13]. For the 1995 run a collimator was placed inside the opening of the PCAL. This determined the geometrical acceptance of the forward spectrometer with angular coverage $-134 < \theta_x < 16$ mr and $-11 < \theta_y < 11$ mr. Fig. 1 shows the acceptance range in proton p_t and rapidity. The vertical acceptance was reduced compared to the E814 configuration in order to limit the multiplicity in the forward spectrometer, since the average multiplicity in Au+Au collisions is approximately 2.5 times higher than in Si+Pb collisions. In order to handle the higher multiplicities, the forward spectrometer was upgraded with a set of four multiwire proportional chambers (MWPC) positioned between the two drift chambers. Also, a new TOF hodoscope, with time resolution of about 80 ps, was installed about 12 meters downstream from the target, behind DC3. Event centrality determination was provided by the calorimeters. The forward spectrometer and the track reconstruction software were capable of tracking up to 25 charged particles per event, though an average event contains only about 7. The momentum resolution was further improved by adding more helium bags, thus reducing the multiple scattering over a larger part of the trajectories in the forward spectrometer. Monte Carlo studies of the momentum resolution showed that it was

better than 3% for protons and pions (see also [13]). This resolution was found to be in good agreement with the momentum dependence of the measured width on the proton mass peak. The corresponding resolution in relative momentum q_{inv} was estimated to be of the order of 7 MeV/c at low relative momenta.

III. DATA ANALYSIS

To determine the two-proton correlation function C_2 experimentally we employ the definition

$$C_2(q_{inv}) = \frac{N_{tr}(q_{inv})}{N_{bk}(q_{inv})} \quad , \quad (1)$$

where

$$q_{inv} = \frac{1}{2} \sqrt{-(p_1^\mu - p_2^\mu)^2} \quad (2)$$

is the half relative invariant momentum between the two identical particles with four-momenta p_1^μ and p_2^μ . The quantities N_{tr} and N_{bk} are the “true” and “background” two-particle distributions obtained by taking particles from the same and different events, respectively. Before constructing the correlation function, several cuts were applied. First, protons were identified using the TOF and momentum measurements. The contamination of other particles in the proton samples is small ($< 2\%$) and is neglected in the following. Beam momentum protons were suppressed by a cut on rapidity $y \leq 3.1$. In order to overcome effects of two-track reconstruction inefficiencies, a cut on the two-track horizontal separation in the drift chambers was applied. The value of the cut has been chosen to be approximately equal to twice the size of the drift cell of a chamber, and was 12 mm and 24 mm for DC2 and DC3, respectively. Monte Carlo studies showed that these cuts effectively suppress distortions due to the close track reconstruction inefficiencies. A requirement that the two protons did not share the same slat of the TOF hodoscope has been imposed on pairs from both distributions. The “background” distribution, N_{bk} , was obtained using an event mixing method. A single proton was selected from one event and then combined with other protons selected from different events to generate the N_{bk} distribution. The large statistics of the N_{bk} distribution ensures that statistical errors in the correlation function are dominated by the statistics of the true proton pairs. The background distribution was normalized such that in a range of q_{inv} from 100 MeV/c to 1000 MeV/c the number of mixed pairs was equal to the number of true pairs.

IV. RESULTS

A. Results for 14.6 A·GeV/c Si+Pb collisions

From one magnetic field polarity setting of the 1991 run, 230k events were selected with a cut on transverse energy corresponding to the upper 10% of the geometric cross section for Si+Pb collisions. The average number of reconstructed protons per event was about 1.4. After all cuts the N_{tr} distribution contains 55k reconstructed proton pairs. Figure 2 shows the rapidity and transverse momentum distributions of the proton pairs for the different ranges of q_{inv} . For each pair, all vectorial quantities (\vec{p} and \vec{p}_t) were defined as an average of two vectors. The rapidity of the pair was defined as the average of rapidities of individual particles. The most important region for correlations, i.e. that with $q_{inv} < 50$ MeV/c, is hatched in the Figure. In order to give a more quantitative characterization of the distributions, Table I shows a summary of the averaged values for the distributions presented in Figure 2. Note that pairs with small q_{inv} are somewhat “softer”, on average, than the rest of the data set. The corresponding correlation function C_2 , as defined by Eq.(1), is plotted in the upper panel of Fig. 3. The error bars reflect only statistical uncertainties. At relative momentum close to 20 MeV/c, a prominent proton-proton resonance peak is evident. The position and the height of the peak is consistent with the E802 preliminary two-proton correlation function [20] measured in 14.6 A·GeV/c Si+Au collisions at $\sigma_{trig}/\sigma_{geom} \approx 0.12$. Note, however, that the E802 measurement was performed at mid-rapidity, while our measurement is at more forward rapidities.

B. Results for 11.5A·GeV/c Au+Au collisions

A total of 47 million events for Au+Au collisions were analyzed. Tracking was performed for those events with transverse energy deposited in the PCAL which corresponds to approximately the most central 22% of the inelastic

cross section. In order to allow direct comparison with the correlation function measured in Si+Pb reactions the correlation function for Au+Au dataset was first determined with the same centrality cut, i.e. for the upper 10% of the inelastic cross section. It can be seen from Fig. 3 that under these conditions the height of the peak of the two-proton correlation function for Au+Au collisions is significantly smaller than in the Si+Pb case, indicating a larger proton source size. Subsequently more cuts on centrality were applied in the correlation analysis. Because of higher statistics in this data set and better momentum resolution it was possible to apply tighter cuts on centrality as well as finer q_{inv} binning for the correlation function. For the purpose of studying the centrality dependence of the correlation function we subdivided the available data into two subsets with different centralities: the most central 4% (14 million events, 5.3 million pairs) and 11%-16% (11 million events, 3.1 million pairs) of the inelastic cross section. Figure 2 shows again the rapidity and transverse momentum distributions of the proton pairs for different ranges of q_{inv} . Table I shows a summary of the average values for the distributions presented in Fig. 2. The definitions of the variables and cuts are identical to those used in Si+Pb data set analysis. The average value of the rapidity distribution is fairly similar for all intervals of q_{inv} . The average rapidity of proton pairs in the less central data set is somewhat higher than the average rapidity of pairs in the most central 4% sample. The average transverse momentum is the same in both subsets. Figure 4 shows the corresponding correlation functions. One trend can be observed here: in the peak region the correlation function for the most central data set (4%) is lower than the correlation function from the less central (11% to 16% centrality) data set. As was discussed in [8] such behaviour is consistent with the assumption of a larger source size in the most central collision. It should be mentioned that the change in the height of the correlation function is determined by the interplay of the changes of the nuclear overlap volume and momentum distributions, which may affect the height of the correlation function in opposite ways. Note that, in a framework of the model discussed in [8,9], the higher average momentum of the proton pairs in the 11 – 16% centrality data should diminish the height of the correlation function, whereas if the source size is smaller in the less central collisions, this would tend to increase the height of the peak of the correlation function.

V. MODEL COMPARISON AND DISCUSSION

In order to extract physical information from the measured correlation functions, we carried out a study using the event generator RQMD(version 1.08) [21,22]. This model describes classical propagation of the particles, together with quantum effects of stochastic scattering and Pauli blocking. It includes color strings, baryon and meson resonances, as well as finite formation time for created particles. It has been successfully used to describe many features of relativistic heavy-ion collisions [5,13,26]. In this model a particle’s freeze-out position is defined as the point of the last strong interaction. The basic structure of our approach to compare model and data is as follows: by taking the freeze-out phase-space distribution generated by RQMD and propagating the particles through the experimental acceptance, accounting for the resolution of the detectors, a subset of the phase-space points was obtained. Then the Koonin-Pratt method [23,24] was used to construct the proton-proton correlation function. This method provides a description of the final state interactions between two protons and antisymmetrization of their relative wave function. The results of the calculations are shown as open symbols in both panels of Fig. 3. One can see that agreement between the experiment and the model is fairly good. Hence, it is of interest to determine the parameters of the proton freeze-out source generated by the RQMD model. The RQMD space-time distributions for 14.6 AGeV/c Si+Pb and 11.5 AGeV/c Au+Au collisions are shown in Fig. 5. All calculations were performed in the nucleon-nucleon center of mass frame and a “top 10%” centrality cut was imposed on model events. The solid-lines and dashed-lines represent the distributions in the experimental acceptance and close to mid-rapidity ($|y - y_{NN}| \leq 1$), respectively. Statistical parameters of these distributions are listed in the Table II. The correlation functions combine the space-time information and it is a non-trivial task to disentangle these related contributions. However, microscopic models provide a valuable insight into these phenomena and several interesting features can be inferred from Fig. 5 and Table II. The space-time parameters for the Si+Pb collisions are smaller than those for Au+Au collisions which is consistent with the measurements shown in Fig. 3 (a bigger source leads to a smaller peak value of the proton correlation function). Since the number of participant nucleons is much larger for the Au+Au collision than for the Si+Pb collision, a higher degree of stopping and higher baryon density are reached for the heavier system. The rescattering in the high density environment will not only bring the system close to the thermal equilibrium, but also develop a strong collective velocity field [14]. The stronger velocity field in the heavier system will naturally lead to a larger final freeze-out space-time extent. Note, we emphasize both space and time variables due to the fact that the two-particle correlation function measures the distance between particles at the instant the second particle is emitted and this distance depends not only on the size of the source but also on the duration of emission. It is instructive to compare the geometrical parameters of the proton source in the model with those of the target and projectile nuclei. The one-dimensional RMS charge radii of the Si and Au projectiles are 1.6 and 3.1 fm, respectively.

From Table II, one can see that all transverse radii (rms value of x-dimension in the Table) are significantly larger than the projectile values for both Si+Pb and Au+Au colliding systems. This observation is consistent with the data from two-pion correlation measurements [5,13] for both colliding systems, which lends further strong support to the interpretation that transverse expansion has occurred in both reactions. It is also consistent with the collective transverse expansion scenario emerging from the study of the systematics of the single-particle transverse momentum distributions¹ [14,15,25–27]. Note that the largest values of the radii in Table II are found at mid-rapidity, consistent with the expectation that, since the highest particle density and collective velocity are both at mid-rapidity, the largest transverse expansion is expected to take place at midrapidity.

VI. CONCLUSION

In summary, we have reported proton correlation functions from Si+Pb and Au+Au central collisions. Model calculations based on RQMD predictions coupled with Koonin-Pratt formalism agree with the data for both systems. Both data and model suggest that the space-time extent for the Au+Au system is larger than that of the Si+Pb system. Combined with the results of centrality dependence studies in Au+Au collisions this confirms that the proton-proton correlation function is sensitive to the number of participants involved in collision. The analysis of model space time distributions leads to a picture consistent with a strong collective expansion in ultrarelativistic heavy ion collisions.

VII. ACKNOWLEDGMENTS

We thank the BNL AGS and tandem operations staff, and Dr. H. Brown for providing the various beams. We also thank Dr. S. Pratt for providing the computer code for the calculation of the correlation. We are grateful to Dr. H. Sorge for making available to us the RQMD source code. This work was supported in part by the U.S. DoE, the NSF, NSERC, Canada, and CNPq, Brazil.

-
- [1] W. Bauer, C.-K. Gelbke, S. Pratt, *Ann. Rev. Mod. Phys.* **42**, (1992).
 - [2] D.H. Boal, C.-K. Gelbke, B.K. Jennings, *Rev. Mod. Phys.* **62**, 553 (1990).
 - [3] T. Abbott *et al.*, E802 Collaboration, *Phys.Lett.* **69**, 1030 (1992).
 - [4] Y. Akiba *et al.*, E802 Collaboration, *Phys. Rev. Lett.* **70**, 1057 (1993).
 - [5] J. Barrette *et al.*, E814 Collaboration, *Phys. Lett. B* **333**, 33 (1994).
 - [6] T. Alber, NA35 and NA49 Collaborations, *Nucl. Phys. A* **590**, 453c (1995); T. Alber *et al.*, *Phys Rev Lett.* **75**, 3814 (1995).
 - [7] H. Beker *et al.*, NA44 Collaboration, *Z. Phys., C* **64**, 209 (1994).
 - [8] S. Koonin, *Phys. Lett. B* **70**, 43 (1977).
 - [9] R. Lednicky, V.L. Lyuboshitz, *Sov. J. Nucl. Phys.* **35**, 770 (1982).
 - [10] A. Mekijan *Phys. Rev. Lett.* **38**, 640 (1977).
 - [11] B. Jennings, D. Boal, J. Shillcock, *Phys. Rev. C* **33**, 1303 (1986).
 - [12] R. Lednicky, V.L. Lyuboshitz, B. Erasmus, D. Nouais, *Phys. Lett. B* **373**, 30 (1996).
 - [13] J. Barrette *et al.*, E877 Collaboration, *Phys. Rev. Lett.* **78**, 2916 (1997).
 - [14] P. Braun-Munzinger, J. Stachel, J.P. Wessels, N. Xu, *Phys. Lett. B* **344**, 43 (1995).
 - [15] I. G. Bearden *et al.*, NA44 Collaboration, *Phys. Rev. Lett.* **78**, 2080 (1997).
 - [16] O. Vossnack, E802 Collaboration, *Proc. Int. Workshop Heavy Ion Physics at the AGS 93*, eds. G.F.S. Stephans, S.G. Steadman and W.L. Kehoe, MITLNS-2158, p. 380.
 - [17] T.C. Awes *et al.*, WA80 Collaboration, *Z.Phys. C* **65**, 207 (1995).

¹For transverse momentum distributions of light particles (π , K, p) it has been found that the slope parameter is a linear function of particle's mass, implying a hydrodynamic-like collective expansion and such dependence is the strongest at mid-rapidity.

- [18] J. Barrette *et al.*, E814 Collaboration, Phys. Rev. Lett. **64**, 1219 (1990).
- [19] J. Barrette *et al.*, E814 Collaboration, Phys. Rev. C **64**, 819 (1992).
- [20] G.S.F. Stephans, E802 Collaboration, Proc. Int. Workshop Heavy Ion Physics at the AGS 93, eds. G.F.S. Stephans, S.G. Steadman and W.L. Kehoe, MITLNS-2158, p. 371.
- [21] H. Sorge, H. Stöcker, and W. Greiner, Nucl. Phys. A **498**, 567c (1989); H. Sorge, R. Mattiello, H. Stöcker, and W. Greiner, Phys. Rev. Lett. **68**, 286 (1992).
- [22] H. Sorge, A. von Keitz, R. Mattiello, H. Stöcker, and W. Greiner, Phys. Lett. B **243**, 7 (1990).
- [23] S. Pratt, Phys. Rev. Lett. **53**, 1219 (1984); S. Pratt *et al.*, Phys. Rev. C **36**, 2646 (1990).
- [24] S. Pratt *et al.*, Nucl. Phys. A **566**, 103c (1994).
- [25] Y. Akiba *et al.*, E802 Collaboration, Nucl. Phys. A **610**, 139c (1996).
- [26] R. Lacasse *et al.*, E877 Collaboration, Nucl. Phys. A **610**, 153c (1996).
- [27] P. Braun-Munzinger and J. Stachel, Nucl. Phys. A **638**, 3c (1998).

TABLE I. Mean values of transverse momentum and rapidity of the proton pairs measured for different colliding systems. See description in the text. The units for p_t are GeV/c.

System	Parameter	$q_{inv} \leq 0.05$ GeV/c	$q_{inv} \leq 0.1$ GeV/c	$q_{inv} \leq 1.0$ GeV/c
Si+Pb	$\langle p_t \rangle$	0.16	0.18	0.21
	$\langle y \rangle$	2.18	2.32	2.34
Au+Au (16%-11%)	$\langle p_t \rangle$	0.35	0.37	0.33
	$\langle y \rangle$	2.56	2.59	2.51
Au+Au (4%)	$\langle p_t \rangle$	0.35	0.36	0.33
	$\langle y \rangle$	2.46	2.50	2.44

TABLE II. Parameters of the proton source calculated using the RQMD model for the Si+Pb and Au+Au systems for different rapidity intervals. All source parameters are in fm.

System	Source Parameters	$-1 < y_{NN} < 1$		In Acceptance	
		Mean	RMS	Mean	RMS
Si+Pb	X	0.0	3.9	0.0	2.5
	Z	-4.2	6.5	5.1	5.8
	$c\tau$	14.	7.3	8.4	6.9
Au+Au	X	0.0	5.7	0.0	4.7
	Z	0.0	7.6	12.7	10.5
	$c\tau$	18.9	8.8	18.3	13.0

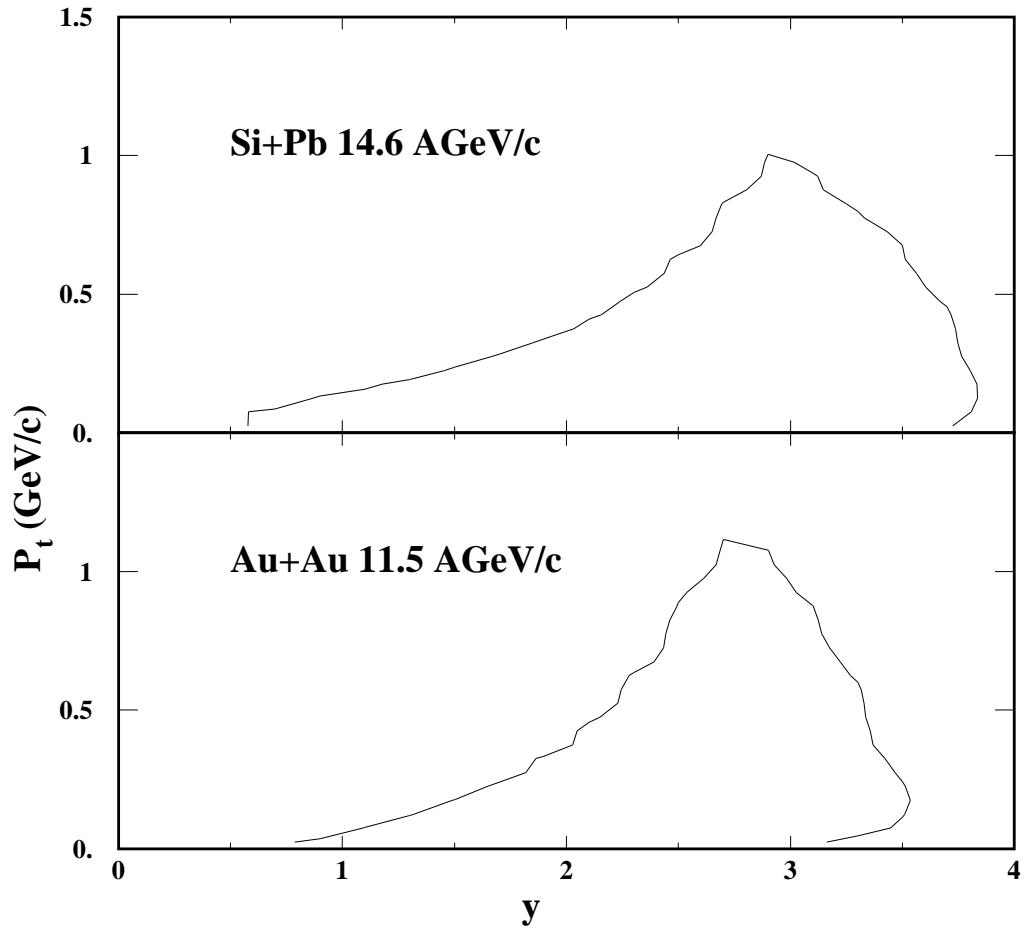


FIG. 1. E814/E877 proton acceptance in the transverse momentum - rapidity ($p_t - y$) plane. Beam rapidities are about 3.4 and 3.1 for Si and Au ions respectively.

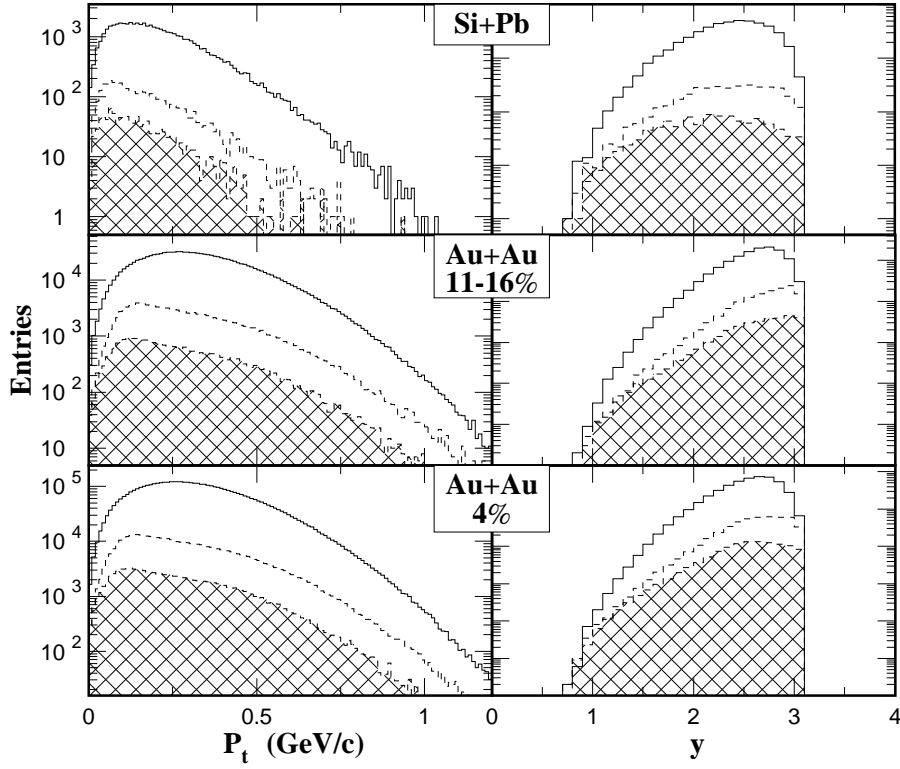


FIG. 2. Transverse momentum (left panels) and rapidity (right panels) distributions of the proton pairs for the different colliding systems. The solid and dashed histograms represent the distributions for pairs with $q_{inv} \leq 1.0$ GeV/c and $q_{inv} \leq 0.1$ GeV/c respectively. Distributions for pairs with $q_{inv} \leq 0.05$ GeV/c are hatched.

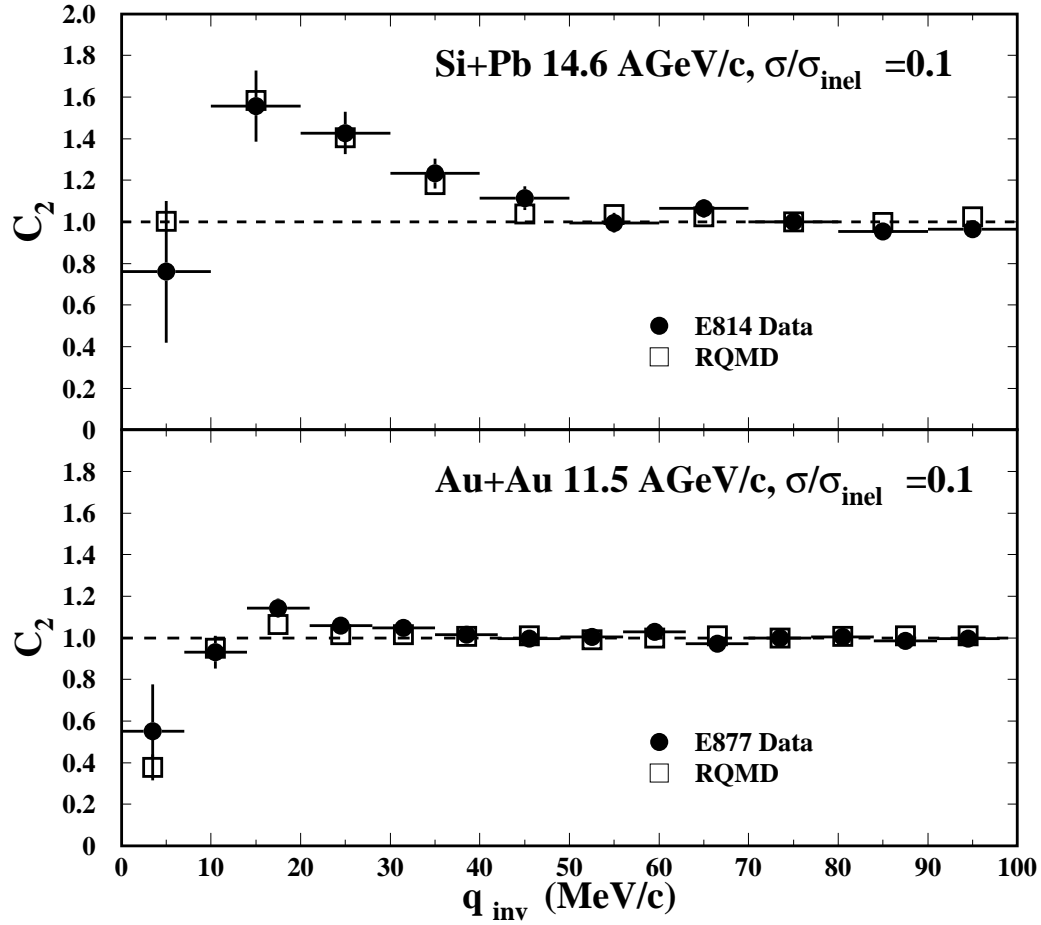


FIG. 3. Two-proton correlation functions for Si+Pb (upper panel) and for Au+Au (lower panel) central collisions. Experimental results are shown as filled circles while the RQMD model predictions are shown as open squares.

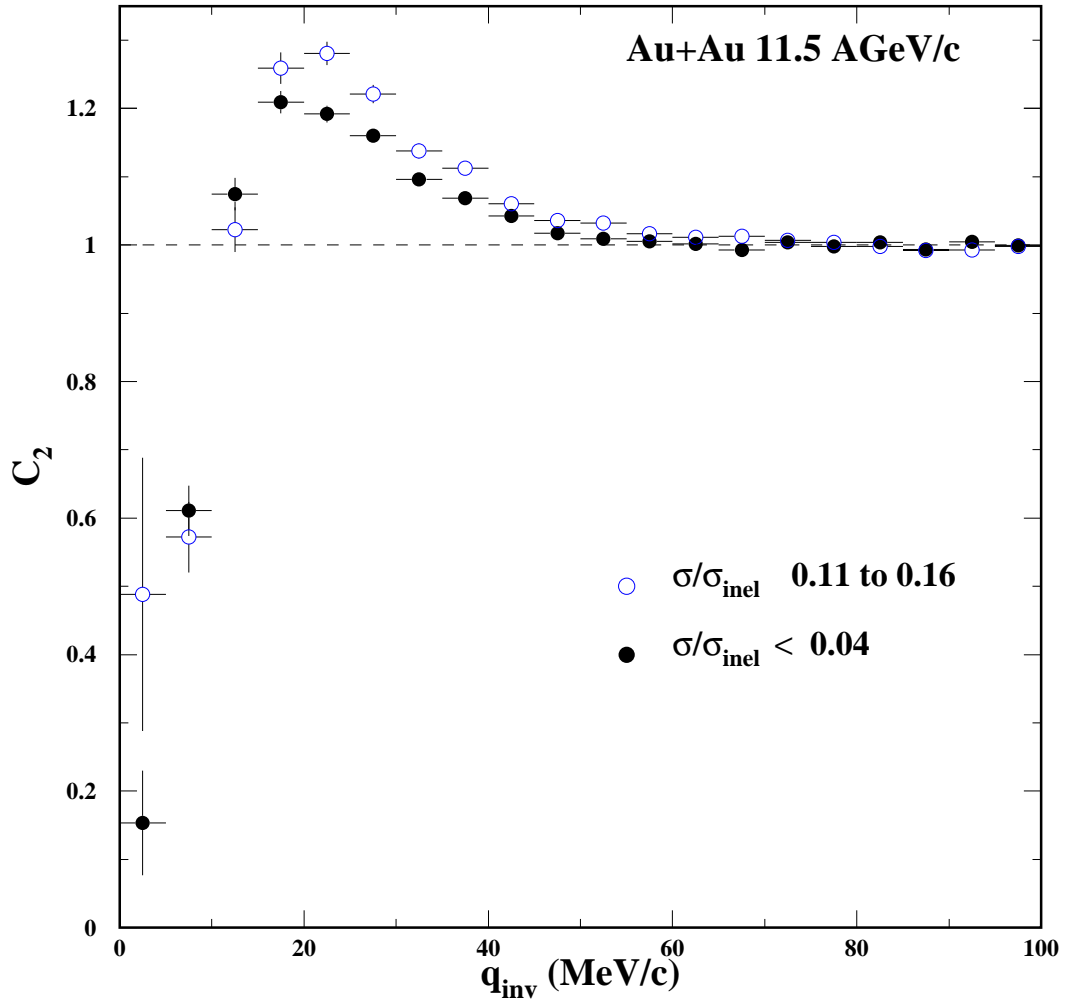


FIG. 4. Two-proton correlation functions for different centralities.

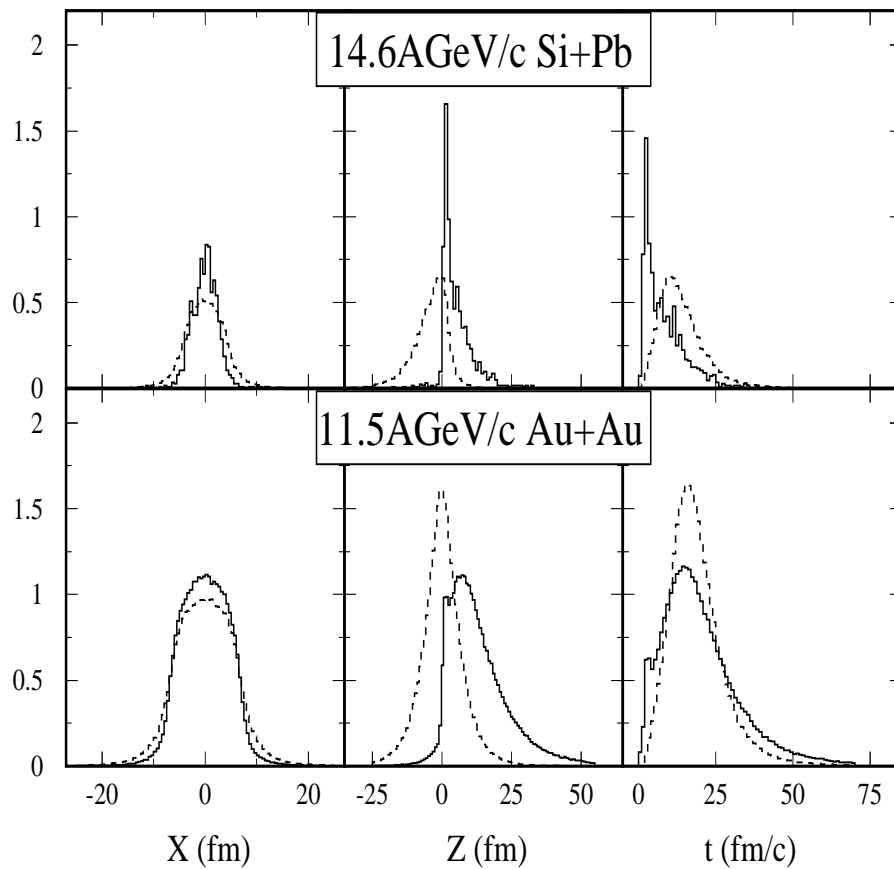


FIG. 5. Proton distributions from RQMD(v1.08). Solid lines represent the distributions of the protons emitted into the E814/E877 spectrometer acceptance; dashed lines represent those at mid-rapidity $-1 \leq y_{NN} \leq 1$